

Synthesis and conformational study in solution and solid state of 1,3-dioxa-6-aza-2(*O*-trimethylsilyl ester)- and 1,3-dioxa-6-aza-2(hydroxy)- $\sigma^4\lambda^4$ phosphacyclooctanes

Cintya Valerio Cárdenas, Virginia Montiel Palma, Miguel-Ángel Muñoz Hernández, and Jean-Michel Grévy*

*Centro de Investigaciones Químicas de la Universidad Autónoma del Estado de Morelos
Avenida Universidad #1001, Colonia Chamilpa, C.P. 62210 Cuernavaca, Morelos México*

E-mail: jeanmichelg@gmail.com

Dedicated to Rosalinda Contreras

Abstract

1,3-Dioxa-6-aza-2 $\sigma^4\lambda^4$ phosphacyclooctane **2** reacts with chlorotrimethylsilane in the presence of triethylamine to afford 1,3-dioxa-6-aza-2(*O*-trimethylsilyl ester) $\sigma^3\lambda^3$ phosphacyclooctane **3**. Compound **3** is readily oxidized with bistrimethylsilylperoxide (BTSP), sulfur and selenium to give the corresponding 1,3-dioxa-6-aza-2(*O*-trimethylsilyl ester) $\sigma^4\lambda^4$ phosphacyclooctane oxide **4a**, sulfide **4b**, and selenide **4c**. The ^1H and ^{13}C NMR analysis in benzene solution show that the heterocycle in **4a-c** adopts the *crown* conformation which is asymmetric due to the restrained amide rotation. The complete proton and carbon assignment of **5c** was completed by running a $^1\text{H}\{^{31}\text{P}\}$ experiment and COSY, NOESY, and HETCOR experiments. The molecular structure of **4b** and **4c** determined by X-ray diffraction are identical and confirm the *crown* conformation. Compounds **4a-c** react with methanol to give the corresponding 1,3-dioxa-6-aza-2(hydroxy) $\sigma^4\lambda^4$ phosphacyclooctane oxide **5a**, sulfide **5b** and selenide **5c**. The NMR analysis of the compounds shows that the heterocycle adopts the crown conformation in DMSO solutions. The crown conformation is also confirmed by the molecular structure of **5a**, determined by X-ray diffraction, which further demonstrates the presence of a strong hydrogen bond between the phosphate hydroxyl and the carbonyl group of neighboring molecules. The existence of this strong intermolecular interaction which leads to the formation of infinite chains for **5a**, is also established for **5b** and **5c** by IR analysis.

Keywords: Phosphoester, heterocycle, dioxazaphosphocane, crown conformation, hydrogen bond, infinite chains, NMR

Introduction

Phosphoester groups are ubiquitous in nature and essential from a biological view point because they are included in the structure of most biochemically important molecules and macromolecules. For example phosphomonoesters can be found substituting some amino acids acting as switches for intracellular signaling (phosphoserine, phosphothreonine, or phosphotyrosine)¹, phosphodiester are present in the nucleic acid backbone as bridges between sugar units or in the polar hydrophilic head group of phospholipids, and phosphoanhydrides in adenosine phosphates stand for energetic resource². Consequently, the transformation of the phosphoester part in those biomolecules and many others is of major interest for pharmaceutical applications and in the design of biochemical tools for biochemistry studies in the laboratory. Within the huge amount of related work, it was previously shown that cyclic ester derivatives of the general structure shown in Figure 1 exhibit general phospholipid properties when R is a lipophilic moiety and also that the phosphonate (R'=H) and phosphate (R'=OH) are respectively agonist and antagonist of the cellular messenger lysophosphatidic acid (LPA)³. However, those eight-membered heterorings, named dioxoazaphosphocanes, are also interesting for conformational aspects and many researchers have worked on determining their ring conformation, the orientation of the exocyclic substituents and the presence of a hypothetical intramolecular transannular interaction between the N and P atoms⁴. Up to this point, the existing NMR and X-ray data analyses show a slight preference for the *chair-chair (crown)* conformation in saturated eight-membered phosphorus heterocycles⁵. On the other hand, the only two X-ray structures of dioxazaphosphocane derivatives reported so far reveal that introducing methyl substituents on the C atoms at ring positions 4 and 8 change the conformation from *crown* to *boat-chair* in the solid state⁶. Those experimental observations were further corroborated in a theoretical study, which not only recognized that the lower energy conformation change from *crown* to *boat chair* under the effect of cyclic C atoms substitution, but additionally established that the *crown* conformation of unsubstituted dioxazaphosphocanes should not be affected by exocyclic substitution with bulky groups at the P and N positions. In order to obtain more answers in the field, we wish to describe here the results obtained in the synthesis and characterization of the oxide, sulfide and selenide derivatives of 1,3-dioxo-6-aza-2-phosphocanes bearing an exocyclic bulky trimethylsilyl ester group, as well as the characterization of phosphate compounds obtained by methanolysis of the corresponding silyl ester derivatives.

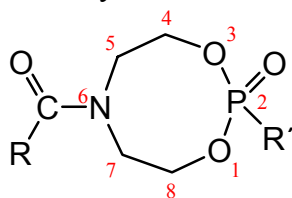
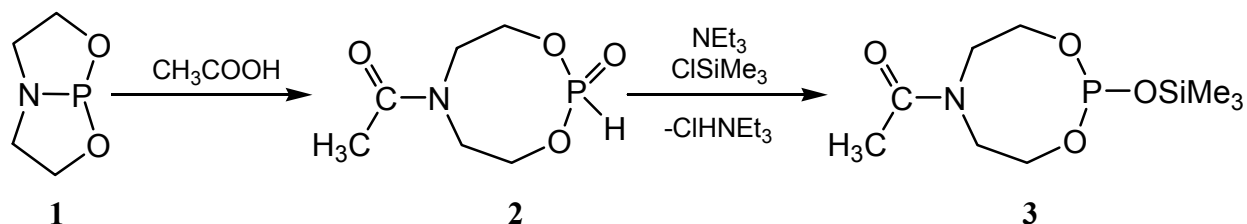


Figure 1. Structure of dioxoazaphosphocanes. When R is a lipophilic moiety (C16 or C18), the phosphonate with R'=H is agonist of LPA and the phosphate with R'=OH is antagonist of LPA.

Results and Discussion

Synthesis of 1,3-dioxo-6-aza-2-(*O*-trimethylsilyl ester) σ^{λ^4} phosphacyclooctanes.

The reaction of bicyclopophane **1** with one equivalent of acetic acid gives the corresponding dioxazaphosphocane **2** as a white solid in nearly quantitative yield after crystallization from toluene (Scheme 1)⁷. This compound can be manipulated for short times on contact with the atmosphere showing that in its P^{IV} state it is quite reluctant to oxidation. However, after one night in refluxing toluene in the presence of a slight excess of triethylamine and one equivalent of chlorotrimethylsilane, the dioxazaphosphocane **2** with a P^{IV} atom is locked into the corresponding trimethylsilyl phosphite **3** with a P^{III} atom, which becomes more sensitive toward oxidation (Scheme 1). Even though this compound was never isolated in pure form, its formation was unambiguously confirmed by a ³¹P NMR analysis of the crude solution where the only signal at δ 129, which is found in the expected region for a phosphite⁸, does not display the typical ¹J_{PH} coupling of 740 Hz observed in **2**. In ¹³C NMR the existence of a coupling between P and the C atoms bonded to O (10.6 and 3.1 Hz) demonstrates that the ring structure is preserved. In addition, it can be concluded that the structure is asymmetric due to the presence of well separated resonances for each ring nucleus in both ¹H and ¹³C NMR analysis (Table 1).



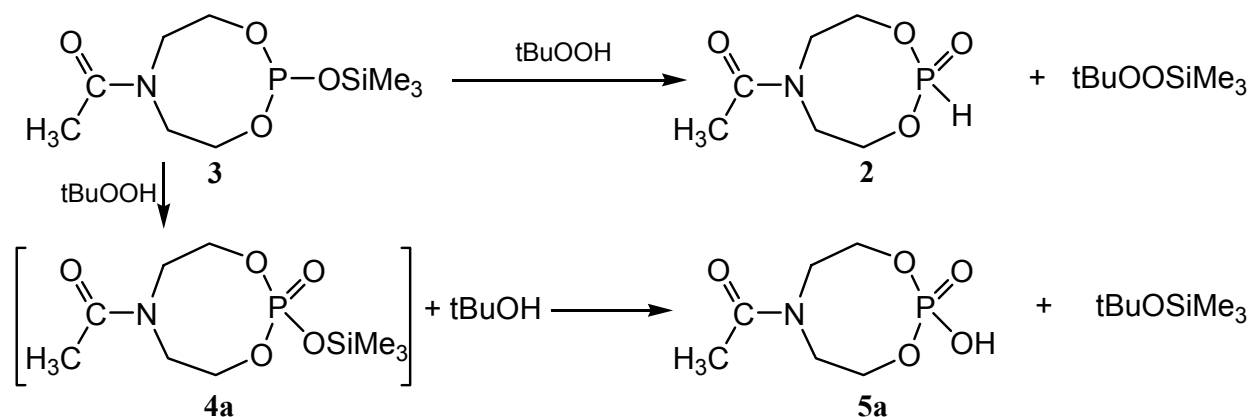
Scheme 1

A first effort to prepare the corresponding oxide by reaction of phosphite **3** with *tert*-butyl hydroperoxide at room temperature lead to a mixture of dioxazaphosphocane **2** and phosphate **5a** identified by their chemical shift in a ³¹P NMR analysis. The ratio of the two signal intensities allowed estimation of the relative proportion **2**:**5a** as 10:90. Although no further studies have been undertaken, it is quite reasonable to presume that compound **2** comes through direct silylation of the oxidant by phosphite **3** and that compound **5a** is obtained in two successive steps where the expected oxide **4a**, obtained at first, subsequently silylates the *tert*-butyl alcohol byproduct of the oxidation (Scheme 2). At this stage it was assumed that dropping the reaction temperature could influence the proportion of the two compounds in the favor of **5a**, but a reaction performed at -78°C afforded **2** in nearly quantitative yield. Owing to difficulties in separating those compounds, it became necessary to look for an oxidant that contained no labile hydrogen so neither the oxidant itself nor the byproduct would interfere with the silylated phosphoester group. Bistrimethylsilylperoxide (BTSP), which is readily obtained by silylation of commercial hydrogen peroxide⁹, was found to be the oxidant of choice. Its reaction with

phosphite **3** in toluene lead to the expected oxide derivative **4a** in quantitative yield with the formation of the volatile hexamethyldisiloxane as the only byproduct (Scheme 3). In ^{31}P NMR the white solid obtained by crystallization from toluene at 4°C shows only one signal at $\delta - 7$ which is within the characteristic region for a phosphoric triester. So, replacing the phosphonate H in **2** by the bulky OSiMe_3 phosphoester group in **4a** generates a 12.6 ppm upfield shift in ^{31}P NMR certainly owing to both electronic and steric changes.

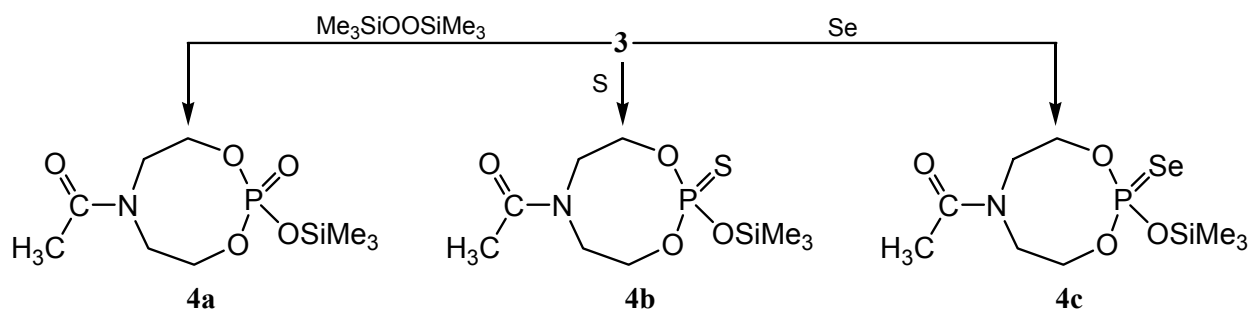
Table 1. ^{31}P , ^1H and ^{13}C NMR chemical shifts of compounds **2**, **3**, **4a-c** in C_6D_6 (400 MHz) and **5a-c** in DMSO D_6 (200 MHz) given in ppm. * Data of compound **2** were taken from the literature⁶

	P		SiMe ₃		CH ₃		CH ₂ O		NCH ₂		C=O
	$\delta^{31}\text{P}$	$\delta^1\text{H}$	$\delta^{13}\text{C}$	$\delta^1\text{H}$	$\delta^{13}\text{C}$	$\delta^1\text{H}$	$\delta^{13}\text{C}$	$\delta^1\text{H}$	$\delta^{13}\text{C}$	$\delta^{13}\text{C}$	
2*	5.6			2.03	21.80	4.57/3.88	64.38	3.31/3.72	50.80	171.20	
						4.39/3.95	64.25	3.08/3.95	50.20		
3	129	0.19	1.98	1.67	22.22	4.09/3.46	61.66	3.84/2.79	51.38	170.01	
						3.96/3.37	60.17	2.96/2.49	50.32		
4a	- 7.0	0.20	1.02	1.64	22.01	4.61/3.77	67.55	3.70/2.68	52.17	170.15	
						4.08/3.38	67.47	2.74/2.46	51.08		
4b	62.7	0.23	1.05	1.66	21.78	4.85/3.70	68.27	3.79/2.46	52.38	170.26	
						4.29/3.35	68.17	2.71/2.39	51.51		
4c	60.3	0.25	1.15	1.69	21.89	4.88/3.65	68.84	3.81/2.42	52.35	170.31	
						4.36/3.32	68.67	2.71/2.38	51.55		
	P	OH		CH ₃		CH ₂ O		NCH ₂		CO	
5a	- 0.6	9.8 (broad)		1.99	21.73	4.07	66.30	3.53	50.83	170.09	
							65.13		48.96		
5b	64.3	8.0 (broad)		1.95	22.40	4.15/3.75	68.06	4.00/3.20	52.00	170.88	
							66.89	3.10	50.45		
5c	63.3	9.3 (broad)		1.95	22.45	4.19/3.75	68.55	4.01/3.20	51.76	171.00	
							67.42	3.10	50.13		



Scheme 2

Oxidation of **3** with elemental sulfur was straightforward and after one night of reaction in toluene at room temperature the sulfide **4b** was obtained in quantitative yield. Oxidation with selenium required reflux conditions to be complete and conversion to selenide **4c** was also quantitative. The compounds crystallized as white solids from toluene and their ^{31}P NMR analysis shows a single signal in the expected chemical shift region for sulfide and selenide phosphoric triesters, *i. e.* δ 62.7 and δ 60.3 respectively. The value of 959 Hz for the direct spin-spin coupling constant between ^{31}P and ^{77}Se indicates the presence of a double P=Se bond in **4c**¹⁰.



Scheme 3

^1H and ^{13}C NMR analysis 1,3-dioxa-6-aza-2(*O*-trimethylsilyl ester) $\sigma^4\lambda^4$ phosphacyclo octanes

In deuterated benzene solutions at room temperature compounds **4a-c** show similar ^1H NMR spectra, almost identical in the case of **4b** and **4c** for which chemical shift differences of a specific proton or group of chemically equivalent protons are less than 0.06 ppm from one spectrum to the other. This means that the nature of the doubly bonded atom to P has no influence on the ^1H NMR of the ring and consequently on its conformation in solution. An important feature, common to the three compounds, is that all 8 cyclic methylene protons are chemically

unequivalent and form two systems, ABKLX and A'B'K'L'X with X being P (Table 1). A COSY spectrum of the methylene region of **4c** in benzene allows to unambiguously identify the signals belonging to each system (Figure 2) even for the overlapped signals L and L'. Additionally, the simplification of AB (δ 4.88 and 3.65) and A'B' (δ 4.36 and 3.32) resonances in a $^1\text{H}\{^{31}\text{P}\}$ NMR experiment demonstrates that those signals correspond to the methylene groups bonded to O (Figure 3). When the associated coupling constant $^3J_{\text{PH}}$ is calculated, two small values are found for A and A', respectively 10.5 and 11.6 Hz, and two large values for B and B', respectively 31.2 and 28.4 Hz. On the basis of the Karplus¹¹ relationship between dihedral angles and the value of the corresponding vicinal coupling constants it is reasonable to assign A and A' to axial protons, which are expected to form a small HCOP dihedral angle ($\sim 60^\circ$) related to a small $^3J_{\text{HP}}$, and B and B' to equatorial protons which are expected to form a large dihedral HCOP angle ($\sim 180^\circ$) related to a large $^3J_{\text{HP}}$.¹² This is the very same situation already reported in previous studies concerning dioxazaphosphocane **2** where it was shown that this heterocycle adopts a *crown* conformation which is asymmetric at room temperature due to the restrained amide rotation⁶. Consequently, it is reasonable to assume that compounds **4a-c** also adopt the same asymmetric crown conformation in benzene solution at room temperature. This assumption is further supported by previous NMR studies which revealed a symmetric *crown* conformation in solution for dioxazaphosphocanes with, instead of the amide, an amine function in position 6 and no substituents on the C atoms of the heterocycle^{6,13}.

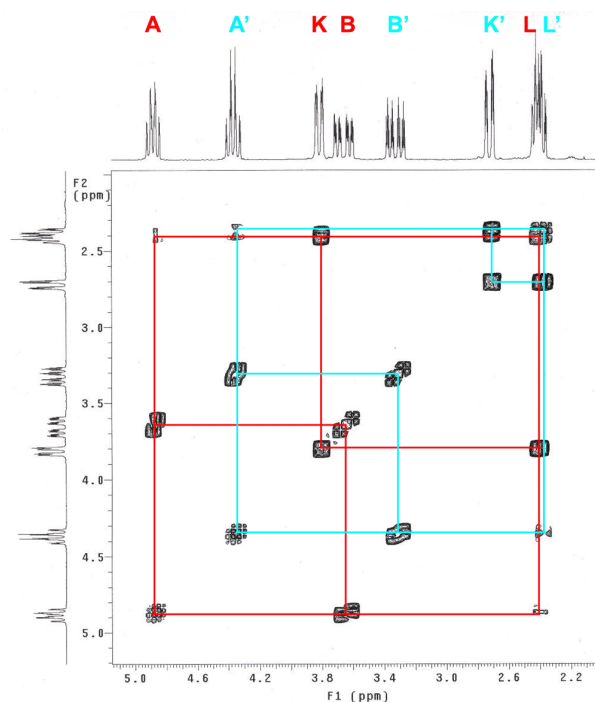


Figure 2. COSY spectrum of the methylene region of **4c** in benzene showing the correlations between protons belonging to the systems ABKLX (red lines) and A'B'K'L'X (blue lines).

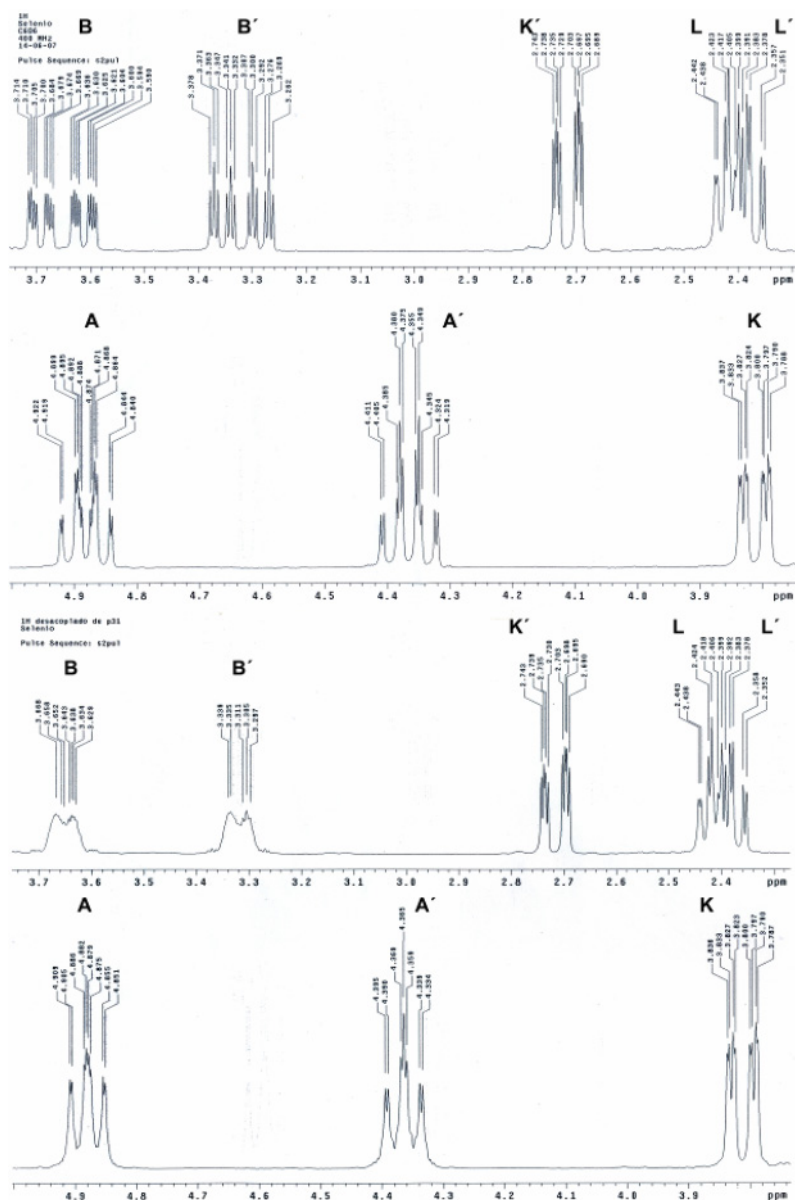


Figure 3. Comparison of ^1H (top) and $^1\text{H}\{^{31}\text{P}\}$ (bottom) NMR spectrum of **4c** in benzene solution. The irradiation at ^1H frequency leads to a simplification of A, B, A' and B' resonances.

In an effort to determine which of the two systems ABKLX and A'B'K'L'X is *cis* or *trans* relative to the methyl of the amide function, a differential NOE experiment was run irradiating at the resonance of the CH_3 protons, but the overlap of L and L' resonances prohibited a clear-cut assignment. It is only through a two dimensional NOESY analysis that the two systems could be assigned. The corresponding spectrum presented in Figure 4 clearly shows NOE correlations between the Me protons of the amide and A' and K' (blue lines), and so indicates that the system A'B'K'L' is in position *cis* relative to the Me amide group. The spectrum also confirm the

previous assumption of A' being axial and B' equatorial, and consequently reveals that K' is equatorial and L' axial. The complete ^1H assignment of **4c** is shown in Figure 5.

The *crown* conformation is further supported by ^{13}C NMR analysis in benzene solution where compounds **4a-c** present very similar spectra. All 4 cyclic carbons are chemically unequivalent and the differences in chemical shift from one spectrum to the other are small (Table 1). The signal multiplicities, as well as the chemical shifts, are also very close to those reported for dioxazaphosphocane **2**⁶ and representative of a single asymmetric *crown* conformation. A HETCOR experiment in benzene solution permits the assignment of the ^{13}C resonances corresponding to the *cis* and *trans* systems relative to amide function (Figure 5). Compared to dioxazaphosphocane **2** the only noticeable difference in ^{13}C NMR of **4a-c** is a 3 to 4 ppm downfield shift of C4 and C8 resonances, certainly due to small changes in the angles of the ring backbone associated with the substitution of one H by the bulky OSiMe₃ group.

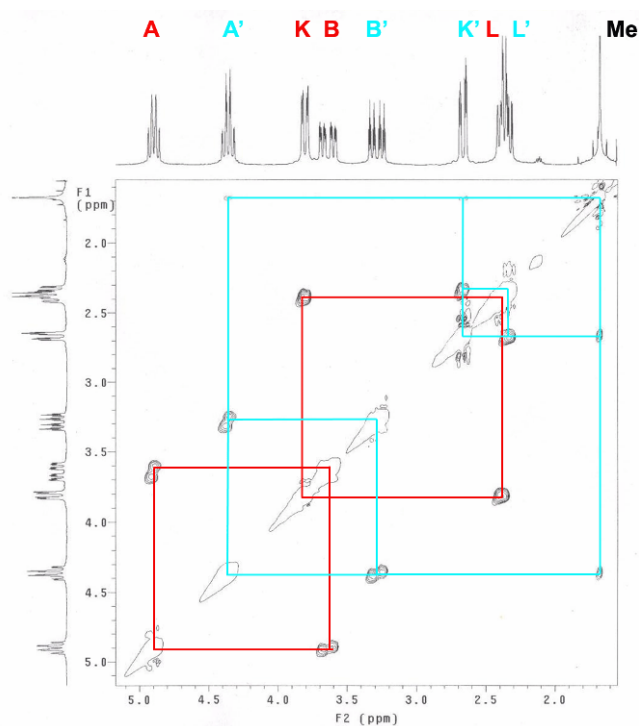


Figure 4. NOESY spectrum of **4c** showing NOE correlations between the Me protons and A' and K' resonances.

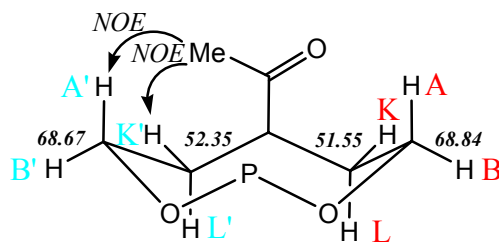


Figure 5. Complete ^1H (ABKL and A'B'K'L') and ^{13}C (ppm in black numbers) assignment of **4c** (for clarity matter the substituents on P are not shown).

X-Ray diffraction analysis of **4b** and **4c**

The structures of **4b** and **4c** were determined by low temperature (100 K) X-ray diffraction studies. Compound **4b** crystallized in the monoclinic P-2(1)/n space group, the corresponding ORTEP molecular diagram is shown in Figure 6, and relevant bond lengths and angles are reported in Table 2. The 8 membered heterocycle adopts a *crown* conformation with the P=S double bond and the exocyclic amide C–N bond in axial positions and eclipsing one another. The geometry at phosphorus is distorted tetrahedral and the phosphorus sulfur distance of 1.92 Å is typical for a P=S double bond in axial position of cyclic phosphotriester sulfide¹⁴. The planarity of the amidic N1 and C5 atoms is clearly shown by the sum of the angles around each atom, respectively 359.8° and 359.9°, and by a carbon nitrogen distance of 1.37 Å, typical for a C–N bond with some double bond character. In addition, a close look to the torsion angles involving the C–N bond and its direct substituents (C2, C3, O4 and C6) reveals that all the atoms belong to a same plane. So, the rotation of the amide function is restrained, providing a configurational diastereoisomerism of the *cis trans* type which consequently clearly accounts for the asymmetry observed in ^1H and ^{13}C NMR studies.

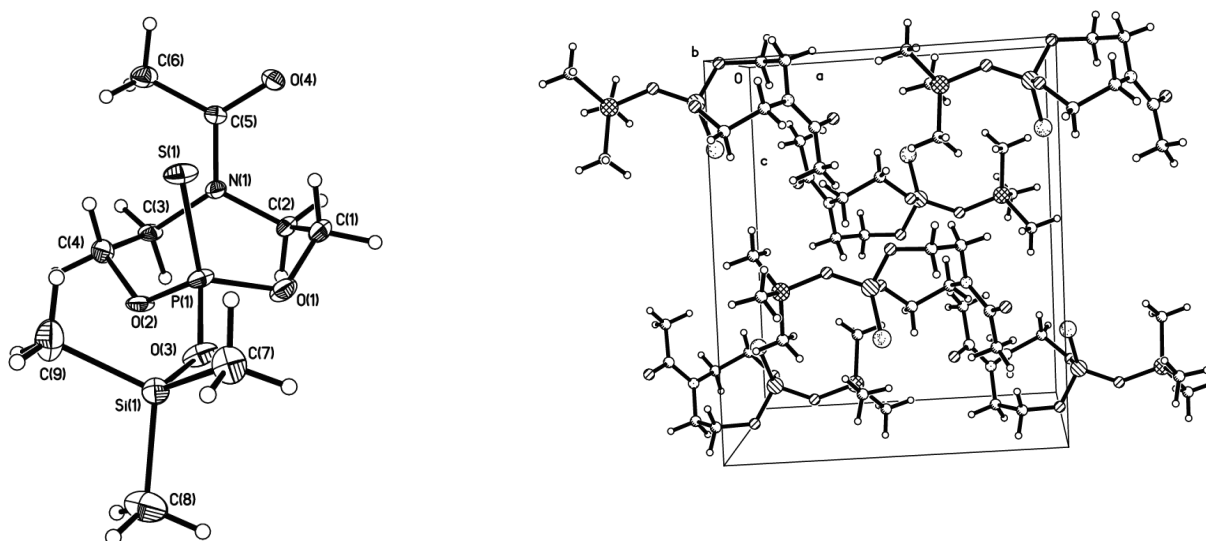


Figure 6. Views of the ORTEP molecular diagram and the unit cell of **4b**.

Table 2. Relevant bond lengths (Å) and bond angles (°) of compound **4b**

Bond lengths [Å]		Bond angles [°]		Torsion angles [°]	
S(1)-P(1)	1.9234(16)	O(1)-P(1)-O(2)	105.70(18)	S(1)-P(1)-O(3)-Si(1)	27.9(4)
Si(1)-O(3)	1.675(3)	O(3)-P(1)-S(1)	118.49(14)	C(3)-N(1)-C(5)-O(4)	-178.0(4)
P(1)-O(3)	1.549(3)	O(1)-P(1)-S(1)	115.98(14)	C(2)-N(1)-C(5)-O(4)	-2.8(6)
P(1)-O(1)	1.582(3)	O(2)-P(1)-S(1)	114.94(13)	C(3)-N(1)-C(5)-C(6)	2.4(6)
P(1)-O(2)	1.586(3)	C(5)-N(1)-C(3)	122.8(3)	C(2)-N(1)-C(5)-C(6)	177.5(4)
O(4)-C(5)	1.236(5)	C(5)-N(1)-C(2)	117.4(3)		
N(1)-C(5)	1.362(5)	C(3)-N(1)-C(2)	119.6(3)		
		O(4)-C(5)-N(1)	120.7(4)		
		O(4)-C(5)-C(6)	121.1(4)		

The analysis of the solid state structure of **4c** (Figure 7) provides exactly the same angles and bond length data with respect to the ring conformation (Table 3), which is *crow*n, and the amide function, which is planar. The phosphorus selenium distance of 2.08 Å is typical for a P=Se axial bond in a cyclic phosphotriester selenide¹⁵. The structures of **4b** and **4c** are not only similar to each other but also very much identical to the one described for dioxazaphosphocane **2** in a previous report⁶, so much identical that a comparison of the three structures in the solid state shows almost no variation in bond lengths and bond angles. The only noticeable difference is found in the intramolecular N1P1 distance, somewhat shorter in **2** (3.18 Å) than in **4b** (3.34 Å) and **4c** (3.33 Å). This particular distance was sometimes used to deduce a transannular interaction between N and P when, as in dioxazaphosphocane **2**, it was found shorter than the sum of the corresponding Van der Waals radii (3.4 Å). Even if this explanation has generated some controversy⁴, it is worth noting here that in the case of **4b** and **4c** the distance between N and P is too long and excludes any hypothetical transannular interaction. Therefore, as it was already observed in solution through NMR analysis, the atom doubly bonded to P (S, Se) and the replacement of the small H in **2** by the bulkier -OSiMe₃ group in **4b** and **4c** have no influence at all on the heterocyclic conformation in the solid state.

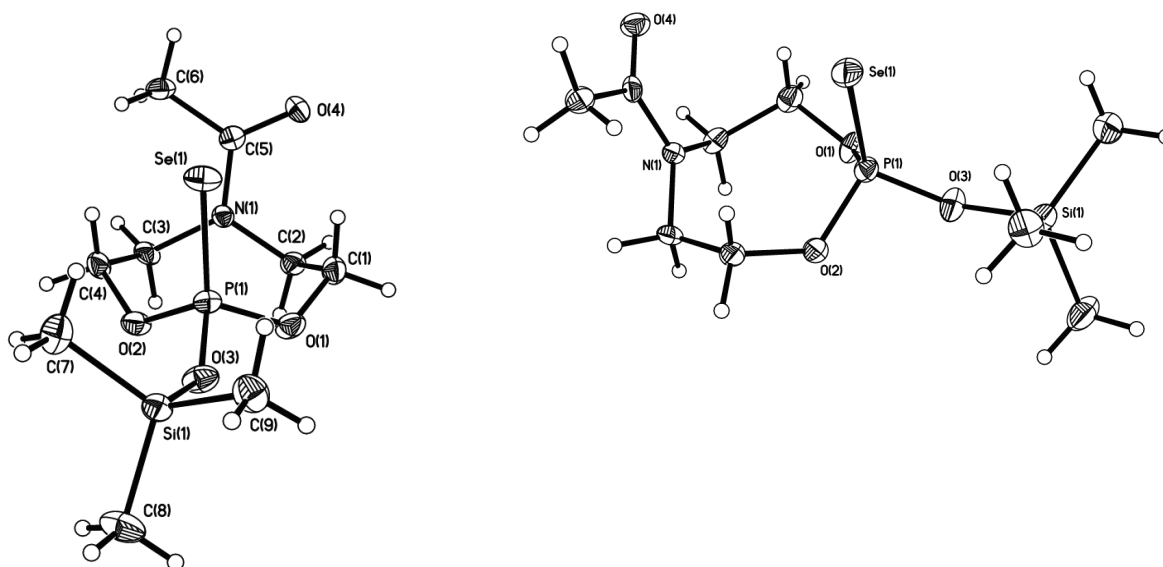


Figure 7. Front view (left) and side view (right) of the ORTEP molecular diagram of **4c**.

Table 3. Relevant bond lengths (Å) and bond angles (°) of compound **4c**

Bond lengths [Å]		Bond angles [°]		Torsion angles [°]	
Se(1)-P(1)	2.0777(10)	O(1)-P(1)-O(2)	105.72(14)	Se(1)-P(1)-O(3)-Si(1)	25.4(3)
Si(1)-O(3)	1.685(2)	O(3)-P(1)-Se(1)	117.96(10)	O(4)-C(5)-N(1)-C(3)	-176.9(3)
P(1)-O(3)	1.550(2)	O(1)-P(1)-Se(1)	115.91(10)	O(4)-C(5)-N(1)-C(2)	-1.2(5)
P(1)-O(1)	1.578(3)	O(2)-P(1)-Se(1)	115.29(9)	C(6)-C(5)-N(1)-C(3)	3.0(5)
P(1)-O(2)	1.584(3)	C(5)-N(1)-C(2)	117.5(3)	C(6)-C(5)-N(1)-C(2)	178.7(3)
C(5)-O(4)	1.231(4)	C(5)-N(1)-C(3)	122.8(3)		
C(5)-N(1)	1.367(4)	C(2)-N(1)-C(3)	119.5(3)		
		O(4)-C(5)-N(1)	120.4(3)		
		O(4)-C(5)-C(6)	121.5(3)		

Synthesis of 1,3-dioxa-6-aza-2-(hydroxy) $\sigma^4\lambda^4$ phosphacyclooctanes

The reaction of compounds **4a-c** with one equivalent of methanol in benzene immediately affords the corresponding phosphate derivatives **5a-c** which precipitate as white solids (Scheme 4).

X-Ray diffraction study of **5a**

A molecular structure determination of **5a** was carried out by X-ray diffraction on a suitable crystal obtained from toluene. Preliminary examination showed that compound **5a** crystallized in the monoclinic system and space group P-2(1)/n. The corresponding ORTEP molecular diagram is shown in Figure 8, and relevant bond lengths and angles are reported in Table 4. The structure of **5a** is basically the same as was described for **4b** and **4c**. The heterocycle adopts a *crown* conformation with the P=O double bond and the exocyclic amide C–N bond occupying axial positions and eclipsing one another. The geometry at phosphorus is distorted tetrahedral and the exocyclic P=O and P–O bond distances, respectively 1.46 and 1.54 Å, are typical for a double bond in axial position and a single bond in equatorial position of a cyclic phosphotriester oxide. The amidic group is planar as seen by the sum of the angles around N1 and C5, which are both exactly equal to 360°, and the torsion angles involving the C5–N1 bond and its direct substituents (C2, C3, O4 and C6), which are close to 0° and 180°. The rotation of the amide function is also restrained here, which provides the same *cis trans* configurational diastereoisomerism observed with the other dioxazaphosphocanes. As seen in the first two structures, the distance between N and P found in **4a** is again too large to indicate a transannular interaction between the two atoms.

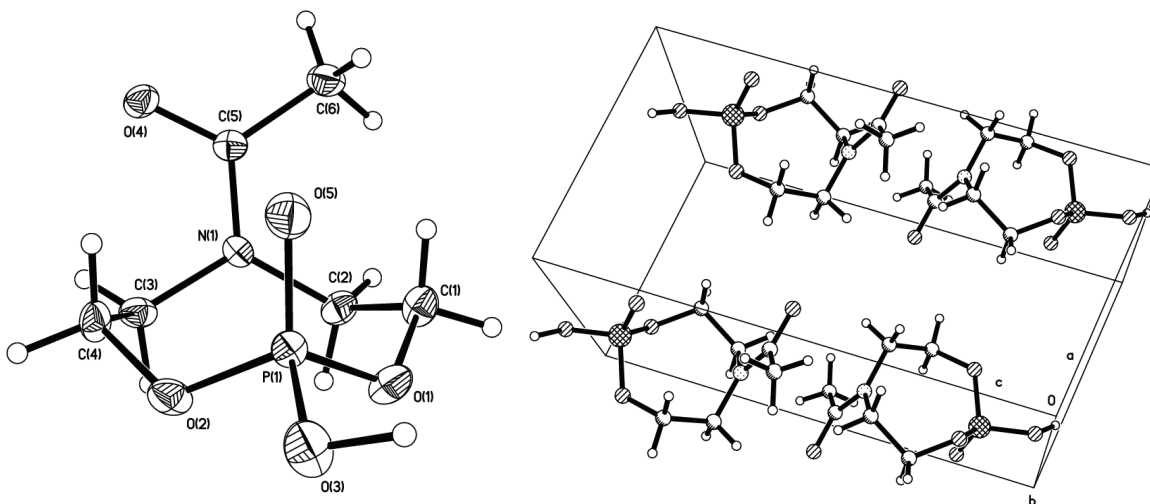


Figure 8. View of the ORTEP molecular diagram and unit cell of compound **5a**.

Table 4. Relevant bond lengths (Å) and bond angles (°) of compound **5a**

Bond lengths [Å]		Bond angles [°]		Torsion angles [°]	
P(1)-O(5)	1.461(3)	O(2)-P(1)-O(1)	105.89(17)	C(3)-N(1)-C(5)-O(4)	-0.1(6)
P(1)-O(3)	1.539(3)	O(5)-P(1)-O(3)	118.52(19)	C(2)-N(1)-C(5)-O(4)	178.0(4)
P(1)-O(2)	1.575(3)	O(5)-P(1)-O(1)	113.23(17)	C(3)-N(1)-C(5)-C(6)	178.3(4)
P(1)-O(1)	1.586(3)	O(5)-P(1)-O(2)	114.33(17)	C(2)-N(1)-C(5)-C(6)	-3.6(6)
O(4)-C(5)	1.250(5)	C(5)-N(1)-C(2)	122.6(3)		
N(1)-C(5)	1.341(5)	C(5)-N(1)-C(3)	117.4(3)		
		C(2)-N(1)-C(3)	120.0(3)		
		O(4)-C(5)-N(1)	119.8(4)		
		O(4)-C(5)-C(6)	119.6(4)		

The solid state structure of **5a** also exhibits the presence of a strong intermolecular hydrogen bonding D–H...A between the phosphate acidic proton and the amidic carbonyl group of neighboring molecules. The distances O3–H5 [$d(D-H) = 1.16(9)$ Å], H5...O4 [$d(H...A) = 1.39(9)$ Å], O3...O4 [$d(D...A) = 2.516(4)$ Å] and the angle O3H5O4 ($163(7)^\circ$) are typical for a strong hydrogen bridge D–H...A between two oxygen atoms^{17,18}. Through this interaction the molecules self organize in a supramolecular assembly of infinite chains ordered in parallel sheets (Figure 9). In one isolated chain the neighbouring heterocycle alternates between upside and downside orientations. In the same sheet the heterocycles of neighbouring chains are oriented tail to tail, while those of neighbouring sheets are oriented head to tail. This strong hydrogen bonding surely accounts for the very low solubility observed for compound **5a** in non polar solvents such as CHCl₃ and benzene. The interaction doesn't affect the conformation of the heterocycle in **5a**, and even the amidic C–N bond length (1.34 Å) and C=O bond length (1.25 Å) are respectively only 0.02 Å shorter and 0.02 Å longer than in **4b** and **4c**.

Although an X-ray diffraction analysis of **5b** and **5c** could not be obtained, the presence in those compounds of a strong hydrogen bond, comparable with that observed in the solid state structure of **5a**, is unambiguously demonstrated by IR spectrum. All three derivatives show IR spectrum with broad bands at 1800 cm^{-1} and between 2000 and 3000 cm^{-1} which are characteristic for a phosphate O–H engaged in strong hydrogen bonding^{16,19}. Additionally, the broadening and shifting to a lower frequency of the C=O absorption ($\Delta\nu \sim 90\text{ cm}^{-1}$) confirm its participation as the acceptor in the hydrogen bonding.

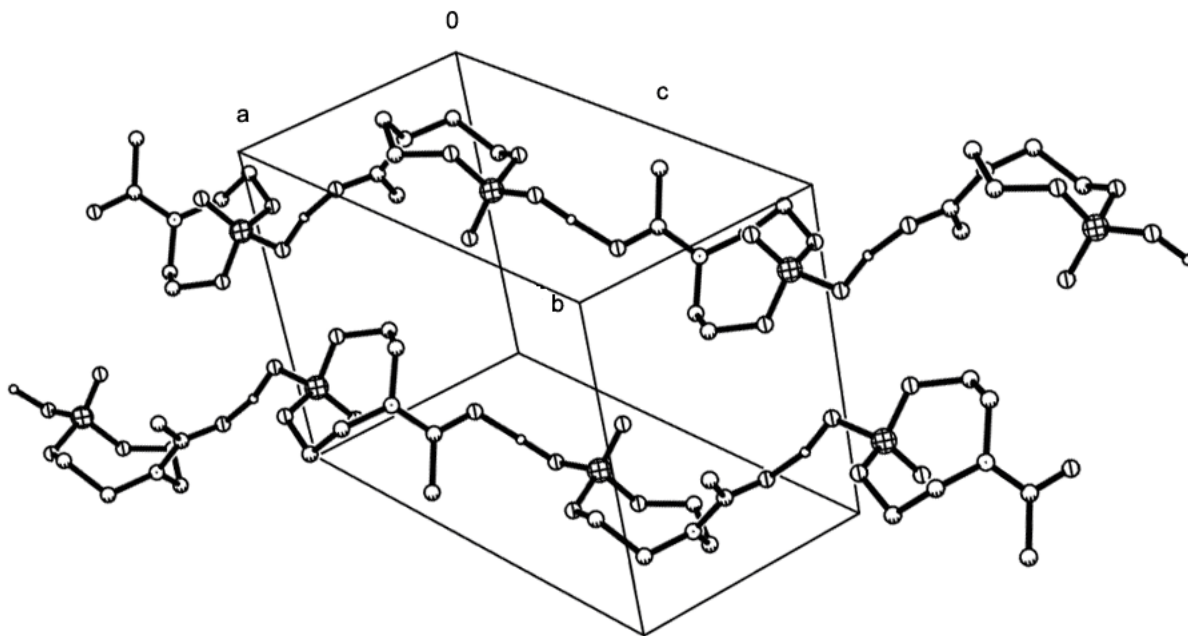


Figure 9. Polymeric chains of **5a** formed through hydrogen bonding between the acidic phosphate proton and the oxygen of the carbonyl amide of neighboring molecules.

Conclusions

The conformation of 1,3-dioxa-6-aza-2(O-trimethylsilyl ester) $\sigma^4\lambda^4$ phosphacyclooctanes without substituents on the cyclic carbon atoms is found to be *crown* and is not influenced by the presence of the bulky trimethylsilyl ester group at phosphorus nor the nature of the atom doubly bonded to phosphorus (O, S, and Se). As shown by the NMR studies in solution the conformation of the eight membered heterocycle is asymmetric due to the restrained amide rotation. The solid state structure of the sulfide and selenide derivatives confirm these observations and show an intramolecular N–P distance which is close to the sum of Van der Waals radii and precludes any transannular interaction. The 1,3-dioxa-6-aza-2-(hydroxy) $\sigma^4\lambda^4$ phosphacyclooctanes obtained by methanolysis of the corresponding trimethylsilyl ester derivatives also show a *crown* conformation in solution when studied by NMR. The molecular structure of the oxide compound (**5a**) reveals a strong hydrogen bonding in the solid state between the phosphate OH and the O of the carbonyl amide group of neighboring molecules [$d(\text{O}\dots\text{O})= 2.516 \text{ \AA}$]. Through this strong interaction the molecules self organize in infinite chains arranged in parallel sheets.

Experimental Section

General Procedures. All syntheses and manipulations were carried out under argon using standard Schlenk line and glove box techniques. Solvents for general use (toluene, hexane, THF, Et₂O) were dried over sodium or potassium/benzophenone and freshly distilled prior to use. Deuterated solvents were obtained from Aldrich, vacuum distilled and stored over molecular sieves. Triethylamine, and chlorotrimethylsilane were purchased from Aldrich and distilled before use. *tert*-butyl hydroperoxide 5.0-6.0M in decane was used as received from Aldrich. The bicycphosphane **1** and dioxazaphosphocane **2** were synthesized according to literature methods.⁷ NMR spectra (¹H, ¹³C and ³¹P) were recorded on Varian-Inova-400 MHz and Varian-Gemini-200 MHz instruments and chemical shifts are reported relative to SiMe₄ for ¹H and ¹³C and are in ppm. Infrared spectra were recorded as KBr pellets on a Bruker Equinox 55 Spectrometer and are reported in cm⁻¹. Microanalyses were obtained on an Elementar Vario EL III instrument operating in the CHN mode.

Single-crystal X-Ray diffraction data for **4b**, **4c** and **5a** were collected using the program SMART²⁰ on a Bruker APEX CCD diffractometer with monochromatized Mo-K α radiation (λ = 0.71073 Å). Cell refinement and data reduction were carried out with the use of the program SAINT, the program SADABS was employed to make incident beam, decay and absorption corrections in the SAINT-Plus v. 6.0 suite²¹. Then, the structures were solved by direct methods with the program SHELXS and refined by full-matrix least-squares techniques with SHELXL in the SHELXTL v. 6.1 suite²². Hydrogen atoms were generated in calculated positions and constrained with the use of a riding model. The final models involved anisotropic displacement parameters for all non-hydrogen atoms. All the refinements were straightforward.

1,3-Dioxa-6-aza-2(*O*-trimethylsilyl ester) $\sigma^3\lambda^3$ phosphacyclooctane (3). Chlorotrimethylsilane (0.565g, 5.2 mmol) was slowly added at room temperature to a stirred mixture of **2** (1g, 5.2 mmol) and 1 equivalent of triethylamine (0.524g, 5.2mmol) in 10 ml of toluene. The reaction mixture was then left under stirring for one night before the white precipitate of triethylamine hydrochloride was filtered off over Celite. A ³¹P NMR analysis of the crude solution showed the presence of only one resonance at 129 ppm. The filtrate was used in the following reactions without further purification considering that the formation of **3** is quantitative. A solution of a crude sample was concentrated and dissolved in deuterated benzene to perform ¹H and ¹³C NMR analysis. ¹H NMR (400 MHz, C₆D₆): δ 0.19 (s, 9H, SiMe₃), 1.67 (s, 3H, CH₃CO) 2.49 (m, 1H) 2.79 (m, 1H) 2.96 (m, 1H) 3.37 (m, 1H) 3.46 (m, 1H) 3.84 (m, 1H) 3.96 (m, 1H) 4.09 (m, 1H) [N(CH₂CH₂O)₂]. ¹³C NMR (100MHz, C₆D₆): δ 1.98 (s, SiMe₃), 22.22 (s, CH₃CON), 50.32 (s, NCH₂), 51.38 (s, NCH₂), 60.17 (d, ²J³¹P¹³C=3.1 Hz, CH₂O), 61.66 (d, ²J³¹P¹³C=10.6 Hz, CH₂O), 170.01 (s, C=O). MS-FAB⁺ *m/z* (%): 266 (100) [MH⁺], 194 (54) [(C₆H₁₂NO₄P)H⁺].

Oxidation of (3) with *tert*-butylhydroperoxide. One equivalent of commercial *tert*-butylhydroperoxide in decane solution (Aldrich) was added drop by drop via a syringe to a

solution of compound **3** in 10 ml of toluene at the desired temperature (25 °C or -78 °C). A sample from the crude reaction mixture was analyzed by ^{31}P NMR after adding few drops of deuterated benzene. Experiment at 25 °C: $^{31}\text{P}\{\text{H}\}$ NMR (81 MHz, C_6D_6) δ [$^1J_{\text{PH}}$]: 6 [740 Hz] (compound **2**, 10%), -0.5 (90%, compound **5a**). Experiment at -78 °C: $^{31}\text{P}\{\text{H}\}$ NMR (81 MHz, C_6D_6) δ [$^1J_{\text{PH}}$]: 6 [740 Hz] (compound **2**, >90%), -0.5 (<10%, compound **5a**).

1,3-Dioxa-6-aza-2-(*O*-trimethylsilyl ester) $\sigma^4\lambda^4$ phosphacyclooctane oxide (4a). The filtrate obtained in the preparation of **3** was then cooled to 0° C (ice bath) and 1 equivalent of BTSP (0.92g, 5.2mmol) was added dropwise by means of a syringe (the reaction is exothermic). The medium was left to come back to room temperature under stirring for one hour and all the volatile compounds were eliminated under vacuum. The solid residue was washed with hexane and dried under vacuum for few hours. Yield: 95%. MP: 58-61 °C. Anal. calcd. for $\text{C}_9\text{H}_{20}\text{NO}_5\text{PSi}$: C, 38.42; H, 7.16; N, 4.98; Found: C, 38.57; H, 7.32; N, 4.83. IR (KBr) ν cm^{-1} : 1644 (C=O). $^{31}\text{P}\{\text{H}\}$ NMR (162 MHz, C_6D_6) δ -7 (s). ^1H NMR (400 MHz, C_6D_6): δ 0.20 (s, 9H, SiMe_3), 1.64 (s, 3H, CH_3CON), 2.46 (m, 1H) 2.68 (m, 1H) 2.74 (m, 1H) 3.38 (m, 1H) 3.70 (m, 1H) 3.77 (m, 1H) 4.08 (m, 1H) 4.61 (m, 1H) [$\text{N}(\text{CH}_2\text{CH}_2\text{O})_2$]. ^{13}C NMR (400 MHz, C_6D_6): δ 1.02 (s, SiMe_3), 22.01 (s, CH_3CON), 51.08 (s, NCH_2), 52, 17 (s, NCH_2), 67.47 (d, $^2J^{31}\text{P}^{13}\text{C}=6$ Hz, CH_2O), 67.55 (d, $^2J^{31}\text{P}^{13}\text{C}=9$ Hz, CH_2O), 170.15 (s, C=O).

1,3-Dioxa-6-aza-2-(*O*-trimethylsilyl ester) $\sigma^4\lambda^4$ phosphacyclooctane sulfide (4b). Elemental sulfur (0.167g, 5.2mmol) was added to the filtrate obtained in the preparation of **3** and the reaction stirred overnight. The medium was then filtered to eliminate any solid material and unreacted sulfur. After reducing the volume of the solution to a few ml, it was stored at 4° C. After few days the product was isolated as colourless crystals. Yield: 96%. MP: 123-125 °C. Anal. calcd. for $\text{C}_9\text{H}_{20}\text{NO}_4\text{PSSi}$: C, 36.35; H, 6.78; N, 4.71; Found: C, 36.60; H, 6.84; N, 4.52. IR (KBr) ν cm^{-1} : 1643.5 (C=O). $^{31}\text{P}\{\text{H}\}$ NMR (162 MHz, C_6D_6): δ 62.7 (s). ^1H NMR (400 MHz, C_6D_6): δ 0.23 (s, 9H, SiMe_3), 1.66 (s, 3H, COCH_3), 2.39 (m, 1H) 2.46 (m, 1H) 2.71 (m, 1H) 3.35 (m, 1H) 3.70 (m, 1H) 3.79 (m, 1H) 4.29 (m, 1H) 4.85 (m, 1H) [$\text{N}(\text{CH}_2\text{CH}_2\text{O})_2$]. ^{13}C NMR (100 MHz, C_6D_6): δ 1.05 (d, $^3J^{31}\text{P}^{13}\text{C}=1.5$ Hz, SiMe_3), 21.78 (s, COCH_3), 51.51 (s, NCH_2), 52.38 (s, NCH_2), 68.17 (d, $^2J^{31}\text{P}^{13}\text{C}=5.3$ Hz, CH_2O), 68.27 (d, $^2J^{31}\text{P}^{13}\text{C}=5.3$ Hz, CH_2O), 170.26 (s, C=O).

1,3-Dioxa-6-aza-2-(*O*-trimethylsilyl ester) $\sigma^4\lambda^4$ phosphacyclooctane selenide (4c). Elemental selenium (0.410g, 5.2mmol) was added to the filtrate obtained in the preparation of **3** and the reaction heated under reflux for 24h. The medium was then cooled to room temperature and filtered to eliminate all solid material and excess selenium. After reducing the volume of the solution to few ml it was stored at 4° C. After few days the product is isolated as colourless crystals. Yield: 92%. MP: 126-128 °C. Anal. calcd. for $\text{C}_9\text{H}_{20}\text{NO}_4\text{PSeSi}$: C, 31.40; H, 5.85; N, 4.07; Found: C, 31.56; H, 5.99; N, 3.88. IR (KBr) ν cm^{-1} : 1643.5 (C=O). $^{31}\text{P}\{\text{H}\}$ NMR (162 MHz, C_6D_6): δ [$^1J(^{31}\text{P}^{77}\text{Se})$] 60.3 [959 Hz]. ^1H NMR (400 MHz, C_6D_6): δ 0.25 (s, 9H, SiMe_3), 1.69 (s, 3H, COCH_3), 2.38 (m, 1H) 2.42 (m, 1H) 2.71 (m, 1H) 3.32 (m, 1H) 3.65 (m, 1H) 3.81 (m, 1H) 4.36 (m, 1H) 4.88 (m, 1H) [$\text{N}(\text{CH}_2\text{CH}_2\text{O})_2$]. ^{13}C NMR (100 MHz, C_6D_6): δ 1.15 (s,

SiMe₃), 21.89 (s, COCH₃), 51.55 (s, NCH₂), 52.35 (s, NCH₂), 68.67 (d, ²J³¹P¹³C= 5.3 Hz, CH₂O), 68.84 (d, ²J³¹P¹³C= 4.5 Hz, CH₂O), 170.31 (s, C=O).

1,3-Dioxa-6-aza-2-(hydroxy)σ⁴λ⁴phosphacyclooctane oxide (5a). To a solution of compound **4a** (500 mg, 1.8 mmol) in 5 ml of toluene at 0 °C, one equivalent of methanol (57 mg, 1.8 mmol) was added under stirring. The white precipitate immediately formed was filtered and dried under vacuum for few hours. Yield: 97%. MP: 130-135 °C. Anal. calcd. for C₆H₁₂NO₅P: C, 34.46; H, 5.78; N, 6.70; Found: C, 34.50; H, 5.90; N, 6.59. IR (KBr) ν cm⁻¹: 1099.27 (P–O), 1241.95 (P=O), 1560.62 (C=O), 1803/2154/2281/2587 (OH, broad). ³¹P{¹H} NMR (81 MHz, DMSO D₆) δ – 0.6 (s). ¹H NMR (200 MHz, DMSO D₆): δ 1.99 (s, 3H, CH₃), 3.53 (m, 4H, NCH₂), 4.07 (m, 4H, CH₂O), 9.8 (broad s, 1H, OH). ¹³C NMR (100 MHz, DMSO D₆): δ 21.73 (s, COCH₃), 48.96 (s, NCH₂), 50.83 (s, NCH₂), 65.13 (d, ²J³¹P¹³C= 6 Hz, CH₂O), 66.30 (d, ²J³¹P¹³C= 6 Hz, CH₂O), 170.09 (s, C=O).

1,3-Dioxa-6-aza-2-(hydroxy)σ⁴λ⁴phosphacyclooctane sulfide (5b). The compound was prepared from **4b** (500 mg 1.7 mmol) and methanol (55 mg, 1.7 mmol) using the same procedure described in the preparation of **5a**. Yield: 95%. MP: 208-211 °C. Anal. calcd. for C₆H₁₂NO₄PS: C, 32.00; H, 5.37; N, 6.22; Found: C, 32.15; H, 5.57; N, 6.04. IR (KBr) ν cm⁻¹: 1093.45 (P–O), 1530 (C=O), 1803.66/2366.15/2649.30 (OH, broad). ³¹P{¹H} NMR (81 MHz, DMSO D₆) δ 64.3 (s). ¹H NMR (200 MHz, DMSO D₆): δ 1.95 (s, 3H, CH₃) 3.10 (m, 1H, NCH₂) 3.20 (m, 1H) 3.75 (m, 2H) 4.00 (m, 2H) 4.15 (m, 2H) [N(CH₂CH₂O)₂], 8.0 (broad s, 1H, OH). ¹³C NMR (50 MHz, DMSO D₆): δ 22.40 (s, COCH₃), 50.45 (s, NCH₂), 52.00 (s, NCH₂), 66.89 (d, ²J³¹P¹³C= 5.7 Hz, CH₂O), 68.06 (d, ²J³¹P¹³C= 6.45 Hz, CH₂O), 170.88 (s, C=O).

1,3-Dioxa-6-aza-2-(hydroxy)σ⁴λ⁴phosphacyclooctane selenide (5c). The compound was prepared from **4c** (500 mg, 1.45 mmol) and methanol (46 mg, 1.45 mmol) using the same procedure described in the preparation of **5a**. Yield: 92%. MP: 192-197 °C. Anal. calcd. for C₆H₁₂NO₄PSe: C, 26.48; H, 4.45; N, 5.15; Found: C, 26.44; H, 4.58; N, 5.02. IR (KBr) ν cm⁻¹: 1090.48 (P–O), 1530 (C=O), 1774.77/2345.73/2591.93 (OH, broad). ³¹P{¹H} NMR (81 MHz, DMSO D₆): δ [¹J(³¹P⁷⁷Se)] 63.3 [894 Hz]. ¹H NMR (200 MHz, DMSO D₆): δ 1.95 (s, 3H, CH₃) 3.10 (m, 1H, NCH₂) 3.20 (m, 1H) 3.75 (m, 2H) 4.01 (m, 2H) 4.19 (m, 2H) [N(CH₂CH₂O)₂], 9.3 (broad s, 1H, OH). ¹³C NMR (50 MHz, DMSO D₆): δ 22.45 (s, COCH₃), 50.13 (s, NCH₂), 51.76 (s, NCH₂), 67.42 (d, ²J³¹P¹³C= 7.2 Hz, CH₂O), 68.55 (d, ²J³¹P¹³C= 7 Hz, CH₂O), 171.00 (s, C=O).

Supplementary Information Available

The supplementary crystallographic data have been deposited at the Cambridge Crystallographic Data Centre and allocated the deposition numbers CCDC 658244 (for **4b**), CCDC 658245 (for **4c**) and CCDC 658246 (for **5a**).

These data can be obtained free of charge at <http://www.ccdc.cam.ac.uk/conts/retrieving.html> (or from the Cambridge Crystallographic Data Centre, 12 Union Road, Cambridge CB2 1EZ, UK; Fax: + 44-1223-336-033; e-mail: deposit@ccdc.cam.ac.uk).

Acknowledgements

This work was generously supported by the Mexican *Consejo Nacional de Ciencia y Tecnología* (CONACyT; grant no. J33675-E).

References and Notes

1. Huse, M.; Kuriyan, J. *Cel.* **2002**, 109, 275.
2. Nelson, D. L.; Cox, M. M. *Lehninger Principles of Biochemistry*, W. H. Freeman Fourth Edition 2004, ISBN-10: 0716743396.
3. Gueguen, G.; Gaige, B.; Grevy, J.-M.; Rogalle, P.; Bellan, J.; Wilson, M.; Klæbe, A.; Pont, F.; Simon, M.-F.; Chap, H. *Biochemistry* **1999**, 38, 8440.
4. Zyablikova, T. A.; Ischmaeva, E. A.; Kataev, V. E.; Vereshchagina, Ya. A.; Bazhanova, Z. G.; Il'yasov, A. V.; Terent'eva, S. A.; Pudovik, M. A. *Russ. J. Gen. Chem.* **2004**, 74, 1171.
5. L. Lamandé, Grévy, J. M.; Houalla, D.; Cazaux, L.; Bellan, J. *Tetrahedron Lett.* **1995**, 36, 8201.
6. Houalla, D.; Bellan, J.; Grévy, J.-M.; Lamandé, L.; Jaud, J. *Phosphorus, Sulfur and Silicon* **2000**, 159, 1.
7. Grévy, J.-M.; Bellan, J.; Lamandé, L.; Pujol, A. *Synlett* **1997**, 5, 555
8. Tebby, J. C. *Handbook of Phosphorus -31 Nuclear Magnetic Resonance Data*, CRC Press 1991, ISBN 0-8493-3531-0.
9. P. G. Cookson, P. G.; Davies, A. G.; Fazal, N. *J. Organomet. Chem.* **1975**, 99, C31
10. Stec, W. J.; Okruszek, A.; Uznanski, B.; Michalski, J. *Phosphorus* **1972**, 2, 97
11. Karplus, M. *J. Chem. Phys.* **1959**, 30, 11.
12. Bentrude, W. G.; Setzer, W. N. In *Phosphorus-31 NMR Spectroscopy in Stereochemical Analysis*, Verkade, J. G.; Quin, L. D.; Eds., VCH: Deerfield Beach, FL, 1987; p 365.
13. Sharma, R. K.; Sampath, K.; Vaidyanathaswamy, R. *J. Chem. Research (S)* **1980**, 12
14. Krishnaiah, M.; Jagadeesh Kumar, N.; Narasaiah, T. V. *Z. Kristallogr.* **1997**, 212, 377
15. Clade, J.; Jansen, M. *Z. Kristallogr. New Cryst. Struct.* **2005**, 220, 234
16. Mikolajczyk, M.; Luczak, J. *Chemistry & Industry (London)* **1974**, 17, 701.
17. Kumara Swamy, K.C.; Sudha Kumaraswamy; Praveen Kommana, *J. Am. Chem. Soc.* **2001**, 123, 12642
18. GiUi, P.; Bertolasi, V.; Ferretti, V.; Gilli, G. *J. Am. Chem. Soc.* **1994**, 116, 909
19. Lord, R. C.; Merrifield, R. E. *J. Chem. Phys.* **1953**, 21, 166
20. Sheldrick, G. M. SMART Bruker AXS, Inc., Madison, WI, USA, 2000.
21. Sheldrick, G. M. SAINT-Plus 6.0 Bruker AXS, Inc., Madison, WI, USA, 2000.
22. Sheldrick, G. M. SHELXTL 6.10 Bruker AXS, Inc., Madison, WI, USA, 2000.